

## *Suzaku* observation of Be / X-ray binary pulsar EXO 2030+375

Sachindra Naik and Gaurava K. Jaisawal

Astronomy and Astrophysics Division, Physical Research Laboratory, Ahmedabad 380009, India;  
snaik@prl.res.in

Received 2014 June 25; accepted 2014 August 20

**Abstract** We study the timing and spectral properties of Be/X-ray binary pulsar EXO 2030+375 using a *Suzaku* observation taken on 2012 May 23, during a less intense Type I outburst. Pulsations were clearly detected in the X-ray light curves at a barycentric period of 41.2852 s, which suggest that the pulsar is spinning-up. The pulse profiles were found to be peculiar, e.g. unlike those obtained from the earlier *Suzaku* observation acquired on 2007 May 14. A single-peaked narrow profile at soft X-rays (0.5–10 keV range) changed to a double-peaked broad profile in the 12–55 keV energy range and again reverted back to a smooth single-peaked profile at hard X-rays (55–70 keV range). The 1.0–100.0 keV broadband spectrum of the pulsar was found to be well described by three continuum models described as (i) a partial covering high energy cut-off power-law model, (ii) a partially absorbed power-law with high-energy exponential rolloff and (iii) a partial covering Negative and Positive power law with EXponential (NPEX) continuum model. Unlike the earlier *Suzaku* observation during which several low energy emission lines were detected, a weak and narrow Iron  $K\alpha$  emission line at 6.4 keV was only present in the pulsar spectrum during the 2012 May outburst. Non-detection of any absorption like feature in the 1–100 keV energy range supports the claim of the absence of the cyclotron resonance scattering feature in EXO 2030+375 from the earlier *Suzaku* observation. Pulse-phase resolved spectroscopy revealed the presence of additional dense matter causing the absence of a second peak from the soft X-ray pulse profiles. The details of the results are described in the paper.

**Key words:** pulsars: individual (EXO 2030+375) — stars: neutron — X-rays: stars

### 1 INTRODUCTION

X-ray binaries are known to be strong X-ray emitters and appear as the brightest X-ray sources in the sky. Depending on the mass of their optical companion, X-ray binaries are classified as low mass X-ray binaries (LMXBs) or high mass X-ray binaries (HMXBs). Based on the type of optical companion, the HMXBs are further classified as Be/X-ray binaries (the largest subclass of HMXBs) or supergiant X-ray binaries. Although evolutionary model calculations show that binary systems with a white dwarf and Be star or a black hole and Be star should also exist, observational evidence confirming the existence of such binary systems has not been found (Zhang et al. 2004 and references therein). However, a recently discovered Be/X-ray binary system with a black hole as the X-ray source (MWC 656; Casares et al. 2014) corroborates the model calculations. The X-ray emitting

compact object in most Be/X-ray binaries is generally a neutron star, whereas the optical companion is a B or O-type star that shows Balmer emission lines in its spectra. The neutron star in these binary systems is typically in a wide orbit with moderate eccentricity. The orbital period of these systems is in the range of 16–400 d.

X-ray emission in Be/X-ray binary systems is known to be due to the accretion of mass from the Be circumstellar disk onto the neutron star during the periastron passage. The abrupt accretion of a huge amount of mass onto the neutron star results in strong X-ray outbursts (Okazaki & Negueruela 2001) enhancing the luminosity of the source by a factor of more than  $\sim 10$  or more. Pulsars in these systems show periodic normal (Type I) X-ray outbursts that coincide with the periastron passage of the neutron star and giant (Type II) X-ray outbursts, which do not show any clear orbital dependence (Negueruela et al. 1998). The spin period of these pulsars is found to be in the range of a few seconds to several hundred seconds. The X-ray spectra of these pulsars are generally hard. A fluorescent iron emission line at 6.4 keV is observed in the spectrum of most accretion powered X-ray pulsars. Cyclotron resonance scattering features (CRSFs) have been detected in the broadband X-ray spectrum of some of these pulsars. Detection of a CRSF provides a direct estimation of the surface magnetic field of these objects. For a brief review of the properties of transient Be/X-ray binary pulsars, refer to Paul & Naik (2011).

The transient Be/X-ray binary pulsar EXO 2030+375 was discovered during a giant outburst in 1985 with the *EXOSAT* observatory (Parmar et al. 1989a). Optical and near-infrared observations identified a B0 Ve star as the counterpart of EXO 2030+375 (Motch & Janot-Pacheco 1987; Coe et al. 1988). Using the *EXOSAT* observation during the giant outburst, the spin and orbital period of the binary pulsar were estimated to be 42 s and 44.3–48.6 d, respectively (Parmar et al. 1989a). During the declining phase of the giant outburst, the pulsar was found to be dramatically spinning-up at a timescale of  $-P/\dot{P} \sim 30$  yr. Strong luminosity dependence of the pulse profile of EXO 2030+375 was detected during the giant outburst in 1985 (Parmar et al. 1989b). The pulse profile was characterized by the presence of two peaks, which were separated by a  $\sim 180^\circ$  phase. The strength of the peaks in the pulse profile reversed as the pulsar luminosity decreased by a factor of  $\sim 100$ . This was explained in terms of a change in the pulsar emission from a fan-beam to a pencil-beam as the luminosity decreased, resulting in the interchange in the strength of the main-pulse and inter-pulse. The *Suzaku* observation of the pulsar at the peak of a Type I outburst, however, showed that the shape of pulse profiles was complex due to the presence of prominent dips at several pulse phases (Naik et al. 2013). The dips were found to be strongly energy dependent and were present up to as high as  $\sim 70$  keV. An extensive monitoring of EXO 2030+375 with *BATSE* and *Rossi X-ray Timing Explorer (RXTE)* showed that a normal outburst had been detected for nearly every periastron passage for  $\sim 13.5$  years (Wilson et al. 2005). Using *BATSE* observations of a series of consecutive Type I outbursts of the pulsar, Stollberg (1997) derived the orbital parameters of the binary system.

The spectrum of the pulsar, obtained from the *EXOSAT* observation during the 1985 giant outburst, was described by a composite model consisting of a blackbody component with temperature  $\sim 1.1$  keV and a power law component describing the hard X-ray part (Reynolds et al. 1993; Sun et al. 1994). However, a model consisting of a blackbody and a power-law with an exponential cut-off was required to fit the 2.7–30 keV spectrum obtained from the *RXTE* observation of the pulsar during the 1996 June–July outburst (Reig & Coe 1999). Possible detection of CRSFs at  $\sim 36$  keV (Reig & Coe 1999),  $\sim 11$  keV (Wilson et al. 2008) and  $\sim 63$  keV (Klochkov et al. 2008) in the spectrum of the pulsar have been reported earlier. However, the absence of any such feature in the 1–100 keV spectrum of the pulsar ruled out the earlier suggestions of the detection of the cyclotron line in EXO 2030+375 (Naik et al. 2013). The broadband *Suzaku* spectrum of the pulsar was best fitted with a partial covering high-energy cutoff power-law model. As the pulsar was very bright, several low-energy emission lines were also detected in the spectrum (Naik et al. 2013).

The *Suzaku* observation of the pulsar at the peak of a Type I outburst with a significantly reduced intensity is used for a detailed study of the evolution and luminosity dependence of the absorption

dips and corresponding changes in its spectral features. The results obtained from this study are described in this paper.

Section 2 gives the details of the *Suzaku* observation used in the present work, Section 3 presents the analysis and results obtained from the observation and Section 4 presents discussion and interpretation of the results obtained from our work.

## 2 OBSERVATION

The transient Be/X-ray binary pulsar EXO 2030+375 consistently shows bright Type I X-ray outbursts at each periastron passage of the neutron star. The luminosities of the pulsar at the peak of these Type I outbursts are, however, found to be different. EXO 2030+375 was observed on 2007 May 14 and 2012 May 23 with the instruments onboard *Suzaku* when the pulsar was undergoing X-ray outbursts. During both the *Suzaku* observations, the peak luminosity was significantly different. One-day averaged light curves of EXO 030+375 in 15–50 keV energy range obtained from the Swift/BAT monitoring data from 2006 November 21 to 2008 February 04 (top panel) and 2011 December 05 to 2013 March 09 (bottom panel) covering both the Type I outbursts are shown in Figure 1. The arrow marks in both the panels show the *Suzaku* observations of the pulsar. The results obtained from the 2012 May *Suzaku* observation of the pulsar during a significantly less intense Type I outburst are discussed in this paper. The observation was carried out at the “XIS nominal” pointing position for total exposures of  $\sim 78$  ks and  $\sim 72.5$  ks for the X-ray Imaging Spectrometer (XIS) and Hard X-ray Detector (HXD), respectively. The XIS was operated in the “1/4 window” mode covering a  $17.8' \times 4.4'$  field of view.

*Suzaku*, the fifth Japanese X-ray astronomy satellite, was launched on 2005 July 10 (Mitsuda et al. 2007). It has two sets of detectors which are XIS (Koyama et al. 2007) and HXD (Takahashi et al. 2007). Installed at the focal plane of four X-ray telescopes (Serlemitsos et al. 2007), the XIS consists of three front-illuminated CCD cameras (XIS-0, 2 and 3) and one back-illuminated CCD camera (XIS-1) that are sensitive in the 0.4–12 keV and 0.2–12 keV energy ranges, respectively. The non-imaging instrument HXD acquires data in the 10–70 keV range with Si PIN photodiodes and in the 40–600 keV range with GSO scintillators. Combining XIS with HXD, *Suzaku* covers a broad energy band and can be used for the detailed study of X-ray sources. The publicly available

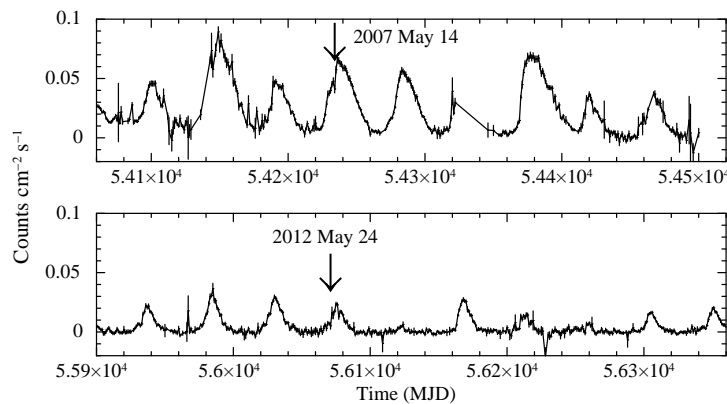


**Fig. 1** *Swift*/BAT light curves of EXO 2030+375 in the 15–50 keV energy band, from 2006 November 21 (MJD 54060) to 2008 February 04 (MJD 54500) and 2011 December 05 (MJD 55900) to 2013 March 09 (MJD 56360) in the top and bottom panels, respectively. The arrow marks in both panels show the date for the *Suzaku* observations of the pulsar during its Type I outbursts.

archival data (version 2.7.16.33) of the 2012 May observation of EXO 2030+375 are used in the present work. As XIS-2 was nonoperational during the above observation of the pulsar, data from the other three instruments that are part of XIS, as well as PIN and GSO, are used in our analysis.

### 3 ANALYSIS AND RESULTS

We used the HEASoft software package (version 6.12) in our analysis. The calibration database files released on 2012 February 10 (for XIS) and 2011 September 13 (for HXD) by the instrument teams were used for data reduction. The unfiltered XIS and HXD event data were reprocessed by using the “*aepipeline*” package of HEASoft. Barycentric correction was applied to the reprocessed XIS and HXD event data by using the “*aebarycen*” task of FTOOLS. These barycentric corrected XIS and HXD event files were used for further analysis. Source light curves and spectra were accumulated from the reprocessed XIS cleaned event data by selecting a circular region with a 3' diameter around the central X-ray source. The background light curves and spectra were extracted from these event data by selecting circular regions away from the source position. “*xisrmfgen*” and “*xissimarfgen*” tasks were used to generate response files and effective area files for corresponding XIS detectors. Hard X-ray light curves and spectra of the pulsar were extracted from the reprocessed HXD/PIN and HXD/GSO event data by using the “*XSELECT*” task of FTOOLS. Simulated background event data for HXD/PIN and HXD/GSO, provided by the instrument team, were used to estimate background light curves and spectra for *Suzaku* observations of the pulsar. Response files released in 2011 June (for HXD/PIN) and 2010 May (for HXD/GSO) and an effective area file released in 2010 May for HXD/GSO were used for spectral analysis.

#### 3.1 Timing Analysis

Source light curves with time resolutions of 2 s, 1 s and 1 s were extracted from the barycenter corrected XIS-0 (in the 0.4–12 keV energy range), PIN (in the 10–70 keV energy range) and GSO (in the 40–200 keV energy range) event data, respectively. As described earlier, the background light curves were extracted from the XIS, PIN and GSO detectors and subtracted from the source light curves. By applying a pulse folding and  $\chi^2$  maximization technique, the spin period of the pulsar was estimated to be 41.2852(3)s. The estimated value of the pulse period of the pulsar showed a global spin-up trend compared with the earlier reported values. Earlier reported values of the spin period of the pulsar at different epochs are tabulated in Table 1. Though episodes of spin-up, spin-down and constant spin frequency are observed at smaller timescales (Parmar et al. 1989a; Wilson et al. 2005, 2008), the pulsar showed an overall spin-up trend over a longer timescale.

The pulse profiles of the pulsar were obtained by folding the background subtracted light curves obtained from XIS, PIN and GSO data with the estimated spin period, and are shown in Figure 2. It can be seen from this figure that the pulse profiles are significantly different in different energy

**Table 1** Global Spin Period History of EXO 2030+375

Date of Observation	MJD	Spin period (s)	References
1985 May 18 – 1985 Nov 03 <sup>a</sup>	46203 – 46372	41.8327 – 41.7275	Parmar et al. (1989a)
1991–2003 <sup>b</sup>	48400 – 52900	41.6910 – 41.6736	Wilson et al. (2005)
2006 June 22 – 2006 Nov 11 <sup>c</sup>	53908 – 54050	41.6320 – 41.4421	Wilson et al. (2008)
2007 May 14	54234	41.4106	Naik et al. (2013)
2012 May 24	56071	41.2852	present study

Notes: <sup>a</sup>: Maximum and minimum values of spin periods out of 13 measurements (table 1 of Parmar et al. 1989a); <sup>b</sup>: Maximum and minimum values of spin periods out of 55 measurements (fig. 1 of Wilson et al. 2005); <sup>c</sup>: Maximum and minimum values of spin periods out of 29 measurements (fig. 4, top panel of Wilson et al. 2008).

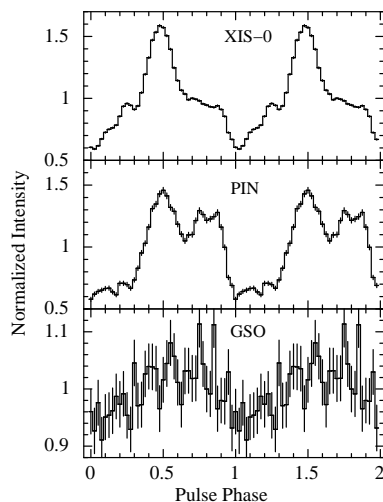


**Fig. 2** Pulse profiles of EXO 2030+375 in the 0.4–12 keV range (XIS-0; *top panel*), 10–70 keV range (PIN; *middle panel*) and 40–200 keV range (GSO; *bottom panel*), obtained from the background subtracted light curves by using the estimated 41.2852 s pulse period. The errors in the figure are estimated with a  $1\sigma$  confidence level. Two pulses are shown for clarity.

ranges. The shape of the pulse profiles obtained from the 2012 May *Suzaku* observation of the pulsar was found to be significantly different compared to that reported from earlier observations (Naik et al. 2013 and references therein). A single-peaked profile in the 0.4–12 keV range (top panel) changed to a structured double-peaked profile in the 10–70 keV range (middle panel) which again became smooth and single-peaked in the 40–200 keV range (bottom panel).

To investigate the evolution of the pulse profile with energy, light curves at various energy ranges were extracted from the XIS, PIN and GSO event data. Background light curves in the same energy ranges were also extracted and subtracted from the corresponding source light curves. Energy resolved pulse profiles were generated by using the estimated spin period of the pulsar and are shown in Figure 3. It can be seen that the pulse profile of the pulsar was single-peaked up to  $\sim 8$  keV, beyond which a hump-like structure appeared after the main peak. The pulse profile became double-peaked up to  $\sim 40$  keV, beyond which it again became single-peaked. The 41.2852 s pulsation was seen in HXD/PIN and HXD/GSO light curves up to the  $\sim 70$  keV range, beyond which it was absent. Though energy dependent pulse profiles are seen in EXO 2030+375, the profiles obtained during the 2012 May outburst are significantly different from those obtained during the 2007 May outburst. Though the observations were carried out during Type I outbursts with the detectors onboard *Suzaku*, the entirely different type of pulse profiles require a detailed spectral investigation to understand the emission mechanism in the pulsar.

## 3.2 Spectral Analysis

### 3.2.1 Pulse-phase-averaged spectroscopy

We carried out simultaneous spectral fitting of the XIS (XIS-0, XIS-1 and XIS-3), PIN and GSO data to investigate the energy dependence of the pulse profile seen in the 2012 May *Suzaku* observation of EXO 2030+375. As described earlier, source spectra were extracted from the XIS, PIN and GSO event data and corresponding background spectra and response files were obtained by following the appropriate procedure. Using the extracted source spectra, background spectra and response files,

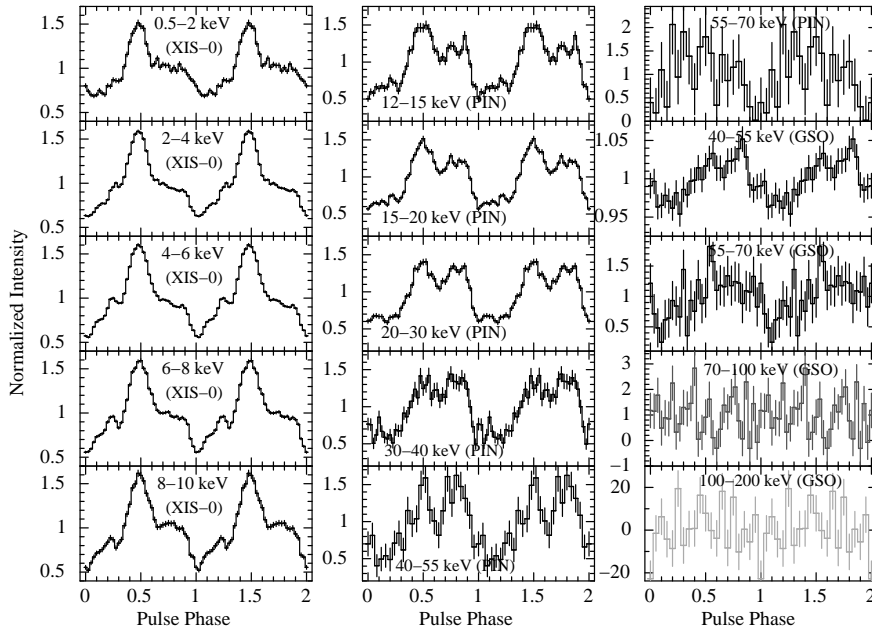


**Fig. 3** Energy-resolved pulse profiles of EXO 2030+375 obtained from XIS-0, HXD/PIN and HXD/GSO light curves at various energy ranges. The presence of absorption dips in profiles at higher energies can be seen in the 0.6–0.8 pulse phase range. The error bars represent  $1\sigma$  uncertainties. Two pulses in each panel are shown for clarity.

simultaneous spectral fitting was carried out using the software package XSPEC v12.7.1. Because of the presence of known structures in the XIS spectra generated by edges from Si and Au in the detector, data in the 1.7–1.9 keV and 2.2–2.4 keV range were ignored from the spectral fitting. XIS spectra were re-binned by a factor of 6 from 1 to 10 keV whereas the HXD/PIN spectra were re-binned by a factor of 4 from 23 keV to 45 keV and by a factor of 6 from 45 keV to 70 keV. The binning of the GSO spectra, however, were done as suggested by the instrument team<sup>1</sup>. In the spectral fitting, all the model parameters were tied together except for the relative instrument normalizations. The broadband energy spectra in the 1–100 keV energy range were fitted with several continuum models such as (i) a high-energy cutoff power-law model, (ii) a power-law with a high energy exponential rolloff, and (iii) a Negative and Positive power law with EXponential cutoff (NPEX) continuum model. The analytical form of the above continuum models is the high energy cutoff power law model –

$$I(E) = \begin{cases} E^{-\gamma}, & (E \leq E_c), \\ E^{-\gamma} \exp\left(-\frac{E-E_c}{E_f}\right), & (E > E_c), \end{cases} \quad (1)$$

where  $E_c$  and  $E_f$  are the cutoff energy and the folding energy, respectively. High energy exponential rolloff model –

$$I(E) = KE^{-\alpha} e^{-E/kT}, \quad (2)$$

where  $K$  is the normalization constant and  $\alpha$  is the photon index.  $kT$  represents the cutoff-energy of a power-law in units of keV. NPEX continuum model –

$$\text{NPEX}(E) = (N_1 E^{-\alpha_1} + N_2 E^{+\alpha_2}) e^{-E/kT}, \quad (3)$$

<sup>1</sup> <http://heasarc.gsfc.nasa.gov/docs/suzaku/analysis/gsobgd64bins.dat>

where  $E$  is the energy of X-ray photons,  $N_1$ ,  $N_2$ ,  $\alpha_1$  and  $\alpha_2$  are normalizations and indexes of negative and positive power-laws, respectively.  $kT$  represents the cutoff-energy of the power-law in units of keV.

Additional components such as photoelectric absorption, and a Gaussian function for an iron emission line, were added to the continuum models while fitting the pulsar spectra. It was found that all the continuum models provided similar fits to the pulsar spectra with a reduced  $\chi^2$  of  $\sim 1.7$ . As in cases of other Be/X-ray binary pulsars, a partial covering absorption component *pcfabs* was then applied to the above continuum models in the spectral fitting. The addition of this component to the above three continuum models improved the spectral fitting, significantly yielding a reduced  $\chi^2$  of  $\sim 1.4$ . The best-fit parameters obtained from the simultaneous spectral fitting to the XIS, PIN and GSO data are given in Table 2. The count rate spectra of the pulsar EXO 2030+375 are shown in Figure 4 (for high-energy cutoff power-law model), Figure 5 (for the power-law with a high energy exponential rolloff model), and Figure 6 (for the NPEX continuum model) along with the model components (top panels) and residuals from the fitted models (bottom panels). In the spectral fitting using the above models, there was no signature of the presence of a CRSF at the earlier reported energies in EXO 2030+375.

**Table 2** Best-fit parameters (with  $1\sigma$  errors) obtained from the spectral fitting of the 1–100 keV spectra of the *Suzaku* observation of EXO 2030+375 during the 2012 May Type I outburst. Model-I, Model-II and Model-III represent the partially absorbed power law with a high-energy cutoff continuum model with interstellar absorption and Gaussian components, a partially absorbed power law with a high-energy exponential rolloff model with interstellar absorption and Gaussian components and a partially absorbed NPEX continuum model with interstellar absorption and Gaussian components, respectively.

Parameter	Value		
	Model-I	Model-II	Model-III
$N_{\text{H1}}$ ( $10^{22}$ atoms $\text{cm}^{-2}$ )	$2.02 \pm 0.02$	$2.02 \pm 0.02$	$1.93 \pm 0.02$
$N_{\text{H2}}$ ( $10^{22}$ atoms $\text{cm}^{-2}$ )	$4.47 \pm 0.15$	$5.16 \pm 0.15$	$4.70 \pm 0.17$
Covering fraction	$0.53 \pm 0.01$	$0.50 \pm 0.01$	$0.44 \pm 0.01$
High energy cut-off (keV)	$6.52 \pm 0.13$	$20.2 \pm 0.4$	$10.6 \pm 0.6$
E-fold energy (keV)	$24.6 \pm 0.5$	–	–
Power-law index	$1.26 \pm 0.01$	$1.07 \pm 0.01$	$0.79 \pm 0.04$
Iron line energy (keV)	$6.41 \pm 0.01$	$6.42 \pm 0.01$	$6.42 \pm 0.01$
Iron line width (keV)	$0.01 \pm 0.01$	$0.03 \pm 0.01$	$0.03 \pm 0.01$
Iron line equivalent width (eV)	$27 \pm 2$	$33 \pm 2$	$33 \pm 2$
1–10 keV flux <sup>a</sup>	$4.5 \pm 0.2$	$4.6 \pm 0.1$	$4.6 \pm 0.2$
10–70 keV flux <sup>a</sup>	$10.6 \pm 0.3$	$10.3 \pm 0.2$	$10.6 \pm 1.4$
Reduced $\chi^2$	1.36 (650 dof)	1.41 (651 dof)	1.38 (650 dof)
Relative Inst. Normalization (XIS-0/XIS-1/XIS-3/PIN/GSO)	1.0/0.94/0.99/1.11/1.06	1.0/0.94/0.99/1.04/1.11	1.0/0.94/0.99/1.11/1.09

Notes:  $N_{\text{H1}}$  = Equivalent hydrogen column density,  $N_{\text{H2}}$  = additional hydrogen column density, <sup>a</sup>: in units of  $10^{-10}$  erg  $\text{cm}^{-2}$   $\text{s}^{-1}$ . Quoted source flux is not corrected for interstellar absorption.

### 3.2.2 Pulse-phase-resolved spectroscopy

Accretion powered transient X-ray pulsars show complex pulse profiles in soft X-ray bands that gradually become smooth and single-peaked at higher energies. As the soft X-ray photons emitted from the polar caps of the pulsar are generally most affected by absorption from matter distributed in the vicinity of the neutron star and in the interstellar medium, the shape of the pulse profiles becomes complex, which is not the case in higher energies. However, the shape of the pulse profiles of EXO 2030+375 obtained from the 2012 May *Suzaku* observation is rather smooth and single-peaked at soft X-rays and complex in higher energies. Therefore, it is interesting to do a detailed spectral

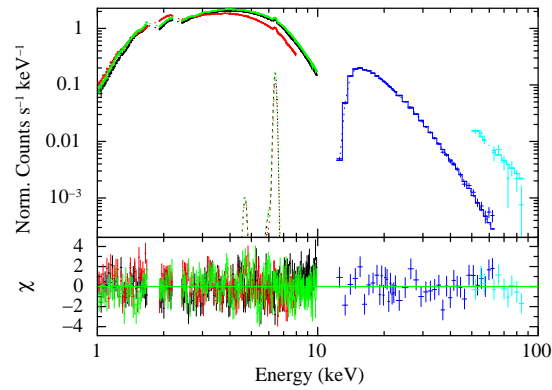


**Fig. 4** Energy spectrum of EXO 2030+375 obtained with the XIS-0, XIS-1, XIS-3, PIN, and GSO detectors of the *Suzaku* observation during the 2012 May-June Type I outburst, along with the best-fit model comprised of a partially absorbed power law with a high-energy cutoff power law continuum model, a Gaussian function for the narrow iron emission line along with the interstellar absorption. The contributions of the residuals to the  $\chi^2$  for each energy bin for the best-fit model are shown in the bottom panel.

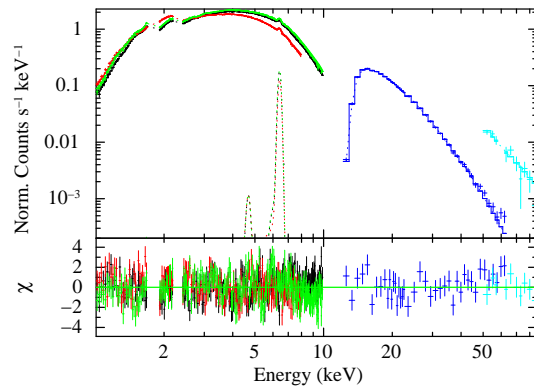


**Fig. 5** Energy spectrum of EXO 2030+375 obtained with the XIS-0, XIS-1, XIS-3, PIN and GSO detectors of the *Suzaku* observation during the 2012 May-June Type I outburst, along with the best-fit model comprised of a partially absorbed power law with the high-energy exponential rolloff model and a Gaussian function for the narrow iron emission line along with the interstellar absorption. The contributions of the residuals to the  $\chi^2$  for each energy bin for the best-fit model are shown in the bottom panel.

study at narrow pulse phases of the transient pulsar during the 2012 May outburst. For the pulse phase resolved spectral study, we used data from XIS (XIS-0, XIS-1 and XIS-3) and HXD/PIN detectors. We did not include HXD/GSO data in phase-resolved spectroscopy because of the lack of a sufficient number of photons at each phase bin of the pulsar. XIS and PIN spectra were accumulated into 20 pulse-phase bins by applying a phase filter in the FTOOLS task XSELECT. Background spectra and response matrices used in the phase-averaged spectroscopy were also used in the phase-resolved spectral analysis. As all three continuum models were yielding similar results while fitting phase-averaged spectra, two of the three models (high-energy cutoff power-law and NPEX continuum models) were used for simultaneous spectral fitting to the phase-resolved spectra in the 1–70 keV

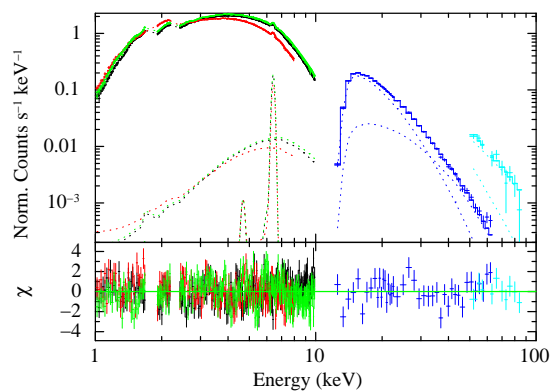


**Fig. 6** Energy spectrum of EXO 2030+375 obtained with the XIS-0, XIS-1, XIS-3 PIN and GSO detectors of the *Suzaku* observation during the 2012 May-June Type I X-ray outburst. The data are plotted with the best-fit model comprised of a partially absorbed NPEX continuum model and a Gaussian function for the narrow iron emission line along with the interstellar absorption. The contributions of the residuals to the  $\chi^2$  for each energy bin for the best-fit model are shown in the bottom panel.

range. In the spectral fitting, the values of relative instrument normalizations were fixed at values obtained from the phase-averaged spectroscopy (as given in Table 2). It was found that certain parameters such as absorption column density ( $N_{\text{H1}}$ ), iron line energy and line width did not show any significant variation over pulse phases of the pulsar. Therefore, these parameters were also fixed at the phase-averaged values.

Parameters obtained from the simultaneous spectral fitting to the phase-resolved XIS and PIN data in the 1–70 keV range are shown in Figure 7. Pulse profiles obtained from XIS and PIN data are shown in the top two panels on both sides of the figure. Parameters obtained from the spectral fitting using partially absorbed NPEX and high-energy cutoff power-law continuum models along with interstellar absorption and a Gaussian function are shown in the left and right panels of the figure, respectively. It can be seen that the parameters obtained from the phase-resolved spectral fitting using two different continuum models followed a similar pattern over the pulse phases of the pulsar. In case of both the models, the value of additional column density ( $N_{\text{H2}}$ ) was found to be high in the 0.6–0.9 pulse phase range. The high value of the additional column density can explain the absence of a significant amount of soft X-ray photons in the above pulse phase range. The absorption of soft X-ray photons by the additional matter makes the pulse profile shallow in the 0.6–0.9 pulse phase range (top panels of Fig. 7). However, at hard X-rays, the effect of the additional matter is drastically reduced making the pulse profile different compared to that in soft X-ray bands. The pulsar spectrum was found to be marginally hard in the 0.8–1.1 phase range along with high values of cutoff energy and iron line equivalent width. This coincides with the presence of a dip (primary dip in the pulse profile) in the pulse profile at this phase range.

#### 4 DISCUSSION

The timing and spectral properties of transient Be/X-ray pulsar EXO 2030+375 have been reported earlier (Naik et al. 2013 and references therein). During normal Type I outbursts, the pulse profile of the pulsar was found to be strongly energy and luminosity dependent. At high luminosity, the pulse profile of the pulsar was found to be complex because of the presence of several prominent narrow dips at various spin phases (Naik et al. 2013). At the low luminosity level, however, the pulse profile was smooth and single-peaked (Parmar et al. 1989b). The strong luminosity dependence of the pulse

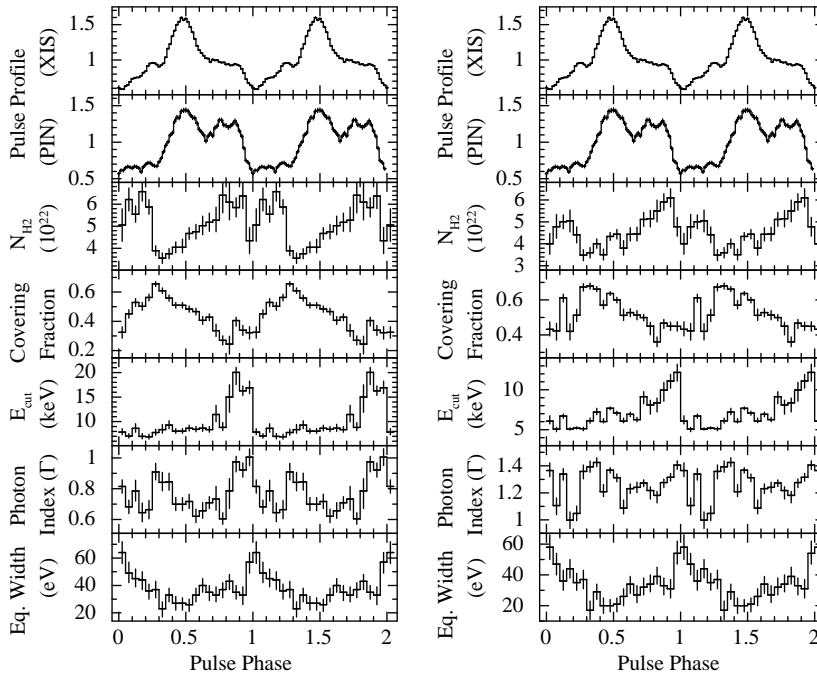


**Fig. 7** Spectral parameters obtained from the pulse-phase-resolved spectroscopy of *Suzaku* observation of EXO 2030+375. The XIS (in the range 0.4–12 keV) and PIN (in the range 10–70 keV) pulse profiles are shown in the top two panels on both sides of the figure. The other panels show the spectral parameters obtained by using a partial covering NPEX continuum model (left panels) and a partial covering cutoff power law continuum model (right panels). The errors shown in the figure are estimated at a  $1\sigma$  confidence level.

profile in EXO 2030+375 has been reported earlier by using observations from several observatories (as discussed in Naik et al. 2013 and references therein). Though the pulsar was observed with *Suzaku* during two Type I outbursts, the shape of the profiles obtained from these observations was significantly different. During the 2007 May Type I outburst, the shape of the pulse profile was complex due to the presence of several energy dependent narrow dips at various pulse phases. The strength of these dips gradually decreased with an increase in energy, making the hard X-ray profile smooth and single-peaked. However, during the 2012 May Type I outburst, the shape of the profile was entirely different – a narrow single-peaked profile at soft X-rays which became a double-peaked profile up to  $\sim 55$  keV beyond which it again became single-peaked. Investigation of the significant difference in the shape of pulse profiles during the 2007 May and 2012 May Type I outbursts may provide information regarding the geometry of the matter distribution around the poles of the neutron star. Accretion of a huge amount of matter onto the neutron star (during bright X-ray outbursts in Be/X-ray binary pulsars) causes changes in the geometry of the matter distribution around the neutron star from a smooth accretion stream to several narrow accretion streams that are phase-locked with the neutron star. These narrow streams of matter cause several absorption dips in the pulse profiles during bright X-ray outbursts. However, when the low mass accretion occurred, the observed pulse profiles are relatively smooth, which is seen in the case of the 2012 May observation of EXO 2030+375 compared to that during the May 2007 outburst.

During the 2007 May *Suzaku* observation, the pulsar was bright in X-ray compared to the 2012 May observation. The source flux in the 1–70 keV range was estimated to be  $\sim 8.9$

$\times 10^{-9}$  erg cm $^{-2}$  s $^{-1}$  (Naik et al. 2013). However, during the 2012 May observation, the pulsar was much fainter with an estimated 1–70 keV flux of  $\sim 1.5 \times 10^{-9}$  erg cm $^{-2}$  s $^{-1}$  (present work). It was also evident from Figure 1 that the 2007 May Type I outburst was much brighter in the 15–50 keV range compared to the 2012 May Type I outburst. While comparing spectral properties of the pulsar, it was found that a partial covering absorption model fitted well to the broadband *Suzaku* spectra during both observations. The value of the absorption column density ( $N_{\text{H1}}$ ) obtained from the spectral fitting was found to be comparable in both cases. However, the value of an additional absorption column density ( $N_{\text{H2}}$ ) was about an order of magnitude higher during the 2007 May observation compared to that during the 2012 May observation. As the pulsar was bright during the 2007 May observation, several narrow emission lines were also detected in the spectrum. A relatively high value of additional absorption column density and the presence of several narrow and prominent absorption dips in the pulse profiles during the high luminosity level of the pulsar indicate accretion of a huge amount of mass from the circumstellar disk of the Be companion star occurred during the 2007 May outburst. The pulse-phase resolved spectroscopy of the 2007 May *Suzaku* observation revealed the presence of narrow streams of matter causing the absorption dips in the pulse profile, which are phase locked with the pulsar. The lower value of additional column density, absence of absorption dips in the pulse profile of the pulsar and about an order of magnitude less luminous during 2012 May *Suzaku* observation confirm that mass accretion from the circumstellar disk of the Be star to the neutron star was significantly low compared to that during 2007 May observation.

In the case of Be/X-ray binary pulsars, it is known that the observed regular and periodic X-ray outbursts during the periastron passage of the neutron star are due to the evacuation of matter from the circumstellar disk of the Be star. Regular monitoring of these Be/X-ray binary pulsars have shown that the peak luminosity of the neutron star during these outbursts varies with time; e.g. in the case of EXO 2030+375, peak luminosity of the pulsar varies by an order of magnitude between the 2007 May and the 2012 May X-ray outbursts. The change in the peak luminosity during the outbursts can be explained as due to the difference in the amount of mass evacuated from the Be circumstellar disk by the neutron star during the periastron passage, which in turn depends on the evolution of the Be circumstellar disk. Therefore, we suggest that the size of the circumstellar disk of the Be star in EXO 2030+375 binary system was relatively small during the 2012 May outburst compared to that during 2007 May observation.

The presence of dips in the pulse profile is seen in many transient Be/X-ray binary pulsars such as A 0535+262 (Naik et al. 2008), GRO J1008–57 (Naik et al. 2011), 1A 1118–61 (Maitra et al. 2012) etc. The evolution of pulse profiles of Be/X-ray binary pulsars from a smooth single-peaked profile (during quiescence) to a complex shape because of the presence of several prominent absorption dips (during Type I outbursts) is briefly described in Paul & Naik (2011) and Naik (2013) and the references therein.

The presence of the absorption dips in the pulse profiles of these transient Be/X-ray binary pulsars is explained as being due to the abrupt accretion of a huge amount of matter that disrupts the accretion stream into several narrow streams of matter that are phase locked with the neutron star. The presence of dips in the pulse profiles of Be/X-ray transient pulsars during Type I outbursts can be compared to the effect of abrupt mass accretion onto weakly magnetized stars. Three-dimensional magnetohydrodynamic simulations of mass accretion from the companion to weakly magnetized stars such as weakly magnetized neutron stars (millisecond pulsars), magnetized white dwarfs in some cataclysmic variables, etc. showed that during an unstable regime of mass accretion, the accreted matter can penetrate into the magnetosphere leading to stochastic light curves (complex pulse profiles), whereas in a stable accretion regime, matter gets accreted in the form of streams yielding almost periodic light curves (Romanova et al. 2008).

In the case of Be/X-ray binary pulsars, a significant amount of mass is being accreted onto the neutron star at the periastron passage, leading to X-ray outbursts. Depending on the amount of mass evacuated from the circumstellar disk of the Be star, the pulse profile of the Be/X-ray binary pulsar

gets modified as seen in the case of EXO 2030+375 – a complex profile because of the presence of several narrow and prominent dips at the high luminosity level and a relatively smooth profile at the low luminosity level. Therefore, the change in shape of the pulse profiles with luminosity in Be/X-ray binary pulsars agrees with the theoretical prediction by Romanova et al. (2008) though it was done for objects with a low magnetic field.

**Acknowledgements** We thank the anonymous referee for his/her useful suggestions that improved the manuscript. The research work at the Physical Research Laboratory is funded by the Department of Space, the Government of India. The authors would like to thank all the members of the *Suzaku* mission for their contributions in the instrument preparation, spacecraft operation, software development and in-orbit instrumental calibration. This research has made use of data obtained through the HEASARC Online Service, provided by NASA/GSFC, in support of NASA High Energy Astrophysics Programs.

## References

- Casares, J., Negueruela, I., Ribó, M., et al. 2014, *Nature*, 505, 378  
 Coe, M. J., Payne, B. J., Longmore, A., & Hanson, C. G. 1988, *MNRAS*, 232, 865  
 Klochkov, D., Santangelo, A., Staubert, R., & Ferrigno, C. 2008, *A&A*, 491, 833  
 Koyama, K., Tsunemi, H., Dotani, T., et al. 2007, *PASJ*, 59, 23  
 Maitra, C., Paul, B., & Naik, S. 2012, *MNRAS*, 420, 2307  
 Mitsuda, K., Bautz, M., Inoue, H., et al. 2007, *PASJ*, 59, 1  
 Motch, C., & Janot-Pacheco, E. 1987, *A&A*, 182, L55  
 Naik, S. 2013, in *Astronomical Society of India Conference Series*, 8, eds. S. Das, A. Nandi, & I. Chattopadhyay, 103 (arXiv: 1308.0411)  
 Naik, S., Maitra, C., Jaisawal, G. K., & Paul, B. 2013, *ApJ*, 764, 158  
 Naik, S., Paul, B., Kachhara, C., & Vadawale, S. V. 2011, *MNRAS*, 413, 241  
 Naik, S., Dotani, T., Terada, Y., et al. 2008, *ApJ*, 672, 516  
 Negueruela, I., Reig, P., Coe, M. J., & Fabregat, J. 1998, *A&A*, 336, 251  
 Okazaki, A. T., & Negueruela, I. 2001, *A&A*, 377, 161  
 Parmar, A. N., White, N. E., & Stella, L. 1989b, *ApJ*, 338, 373  
 Parmar, A. N., White, N. E., Stella, L., Izzo, C., & Ferri, P. 1989a, *ApJ*, 338, 359  
 Paul, B., & Naik, S. 2011, *Bulletin of the Astronomical Society of India*, 39, 429  
 Reig, P., & Coe, M. J. 1999, *MNRAS*, 302, 700  
 Reynolds, A. P., Parmar, A. N., & White, N. E. 1993, *ApJ*, 414, 302  
 Romanova, M. M., Kulkarni, A. K., & Lovelace, R. V. E. 2008, *ApJ*, 673, L171  
 Serlemitsos, P. J., Soong, Y., Chan, K.-W., et al. 2007, *PASJ*, 59, 9  
 Stollberg, M. T. 1997, PhD Thesis, University of Alabama in Huntsville  
 Sun, X.-J., Li, T.-P., Wu, M., & Cheng, L.-X. 1994, *A&A*, 289, 127  
 Takahashi, T., Abe, K., Endo, M., et al. 2007, *PASJ*, 59, 35  
 Wilson, C. A., Fabregat, J., & Coburn, W. 2005, *ApJ*, 620, L99  
 Wilson, C. A., Finger, M. H., & Camero-Arranz, A. 2008, *ApJ*, 678, 1263  
 Zhang, F., Li, X.-D., & Wang, Z.-R. 2004, *ApJ*, 603, 663